Iranian Polymer Journal
https://doi.org/10.1007/s13726-024-01348-z

ORIGINAL RESEARCH

# The degradation of poly(1-butene) extrudates subjected to artificial and natural aging

**Sona Zenzingerova[1] · Michal Kudlacek[1] · Lubomir Benicek[1] · David Jaska[1] · Jana Navratilova[1] · Lenka Gajzlerova[1] · Roman Cermak[1]**

Received: 4 December 2023 / Accepted: 1 May 2024


## Abstract

In this work, we examined the degradation behavior of isotactic poly(1-butene) (PB-1) under artificial aging and natural weathering conditions. PB-1 samples underwent accelerated aging through UV irradiation and natural weathering. Chemical and structural changes in the degraded samples were characterized using Fourier-transform infrared–attenuated total reflectance (FTIR–ATR) spectroscopy, surface analysis, and wide-angle X-ray scattering (WAXS). The mechanical properties were evaluated via tensile testing. FTIR–ATR analysis revealed the presence of carbonyl groups in the degraded samples, indicating oxidative degradation. Surface observations employing scanning electron microscopy (SEM) revealed the formation of surface cracks in both samples, with differing crack initiation mechanisms. The two aging methods affected the mechanical properties of the samples: artificial aging induced a gradual reduction in both tensile modulus and strength, whereas natural weathering engendered a marginal increment in modulus alongside diminished strength. Additionally, elongation-at-break value witnessed a marked decrease in both sample sets during the preliminary stages of degradation. This work employed accelerated time equivalent, obtained by juxtaposition of the values of carbonyl index during both artificial aging and natural weathering and their interpolation to determine the degradation rate and adequately to correlate the final properties of the aged PB-1. It was observed that surface morphology and mechanical attributes of degraded samples were subject to additional influences such as temperature, humidity, and precipitation during natural weathering. This research work provided significant insights into PB-1 degradation mechanisms and effect of different aging conditions on its performance.

✉ Lubomir Benicek
benicek@utb.cz

[1] Department of Polymer Engineering, Faculty of Technology, Tomas Bata University in Zlin, Vavreckova, 5669, 760 01 Zlin, Czech Republic

Published online: 20 June 2024

**Graphical abstract**

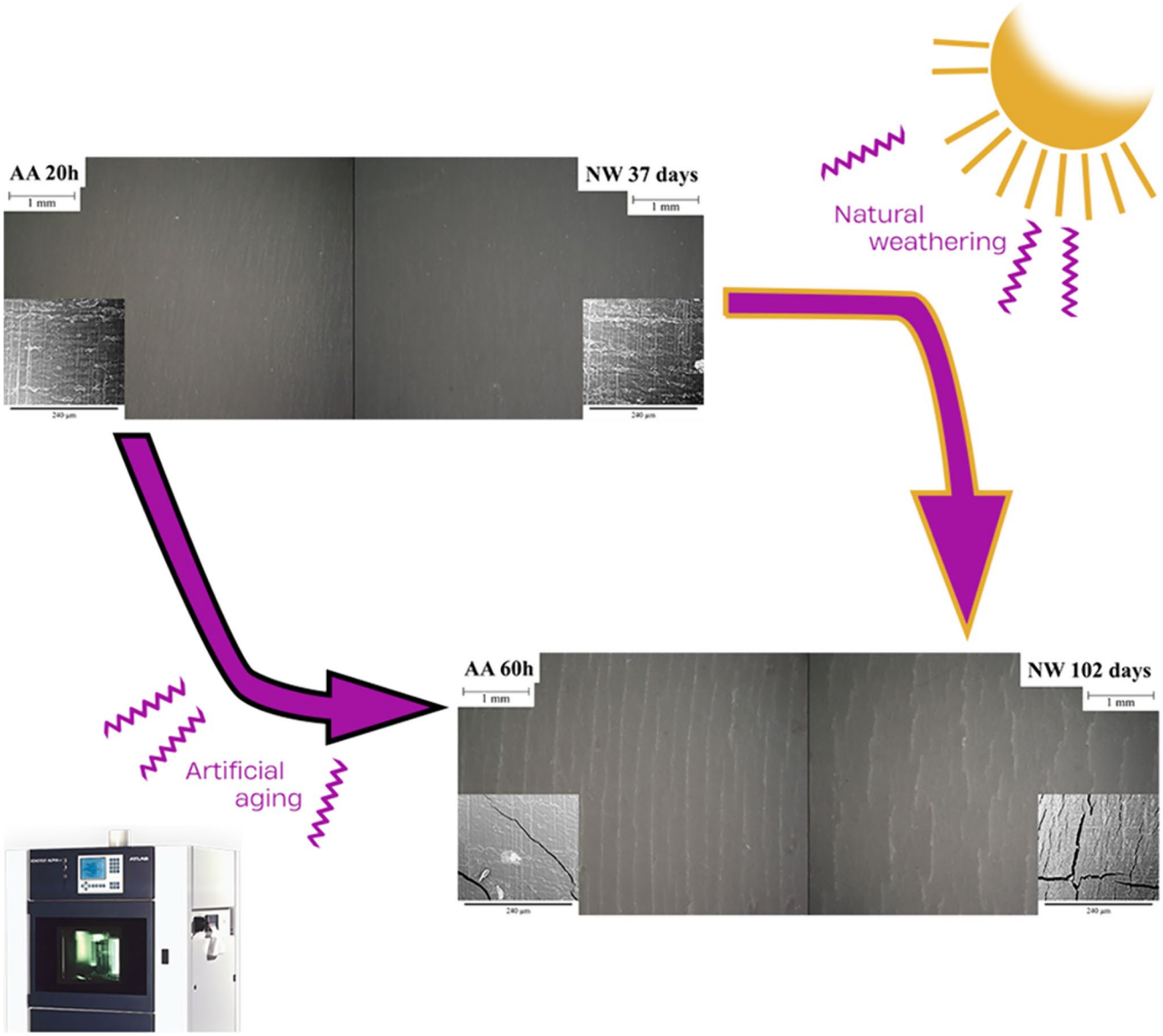


**Keywords** Isotactic poly(1-butene) · Accelerated time equivalent · Degradation · Weathering · Surface changes

## Introduction

Isotactic poly(1-butene) (PB-1) is a thermoplastic polyolefin with remarkable properties, distinguishing it from ordinary polyolefins, such as isotactic polypropylene or polyethylene. Compared to other polyolefins, PB-1 exhibits low stiffness, high creep resistance, good elastic recovery, and exceptional chemical resistance, e.g., to oils, fats, acids, alcohols, and ketones. Equally important is its high heat distortion temperature [1]. The physical, chemical, and mechanical properties are influenced by the given crystalline phase.

Despite its excellent properties, the application of PB-1 compared to other polyolefins is limited by conformational polymorphism and dimensional instability, reaching up to 4%, which occurs during the transition between the initial metaphase II and stable phase I. The individual phases exhibit different densities [2–4]. Four crystalline phases of PB-1 have been characterized thus far. Crystallization from the melt follows Ostwald's rules of stages [5]. Initially, the kinetically favored unstable tetragonal mesophase II is formed from the melt, transforming into the hexagonal phase I within a few days. During the transition between phases II

and I, phase I', which has the same crystal structure as phase I but differs in lower melting temperature, can be formed, probably caused by more conformational defects present. The unstable phase III has an orthorhombic structure and is obtained by solvent evaporation or precipitation, followed by transformation to phase I under certain conditions [6].

Important factors influencing the aging process of polymers include aging time, applied radiation (solar or fluorescent light sources), the presence of oxygen, ozone ($O_3$), applied heat, humidity, rain, impurities in the air, and others. The chemical structure of the polymer chains and morphology determine its resistance to chain degradation. Stable structures with higher density and crystalline regions showed an enhanced resistance to the diffusion of penetrating substances and radiation [7].

However, the course of degradation of PB-1 still needs to be fully understood. This process is assumed to be similar to the degradation of isotactic polypropylene due to identical presence of tertiary carbon in the main chain [8–10]. Craig et al. [11] investigated the oxidation of isotactic polypropylene at room temperature; the polymer was in the solid state and well below its crystallization temperature. Changes occurred primarily in the amorphous region; oxygen can diffuse freely through this area. In contrast, it hardly passes through the crystalline regions. The main changes were (i) chain scission, (ii) cross-linking, and (iii) formation of molecular defects, e.g., formation of carbonyl groups.

During chain scission, the chain segments that were previously entangled were released, and crystallization might occur. If the polymer was formed from many free segments, the formation of new crystals could be assumed, but it is more likely that the segments formed in this way would join the existing growth surfaces. When the crystallinity of the material increases, secondary crystallization occurs, known as the "chemi-crystallization" process [12, 13].

Cross-linking inhibits further crystallization of chain segments connected by networks. Molecular defects such as formed carbonyl groups do not fit into the crystal lattice, and parts of the molecular segments containing such defects cannot participate in secondary crystallization [11, 14, 15].

During the so-called "chemi-crystallization", the amount of low-density amorphous phase increases compared to the crystalline phase; shrinkage of the material occurs. Chain scission (and subsequently secondary crystallization and shrinkage) tends to be highly dependent on the distance from the UV source resulting in residual stresses on the material's surface [16]. Residual and "frozen stresses" arising during processing can lead to material cracking. Fine cracks that are not deep and do not lead to total failure of the material can, among other things, impair the appearance of the material, for example, its gloss.

A material affected by molecular degradation and subsequent loss of mechanical integrity provided by the molecular network exhibits reduced flexibility resulting from increased crystallinity and additional cross-linking [17, 18]. The degradation conditions also influence the degradation behavior [19]. The general factors that can influence or even limit the degradation of polymers are divided into physicochemical conditions and material properties.

Material properties play a significant role, among them thickness of material [20], polymer crystallinity [21], molecular weight [22, 23], or polymer composition [24, 25]. The formation of peroxide substances in the main chain of a polymer is encountered as the primary step of oxidative degradation. Hydroperoxide groups are essential for inducing thermal oxidation and photo-oxidation of polymers, but they are also important intermediates in overall oxidation reactions. Critical physicochemical conditions determined by the environment, include relative humidity [26, 27], pH value [28, 29], temperature [30, 31], amount of UV and visible irradiation [32, 33], or availability of oxygen [34, 35]; therefore, different results in this work would be expected.

Understanding the degradation mechanisms and the impact of degradation conditions on the properties of PB-1 is crucial due to its widespread application in various fields such as geothermal piping, easy-peel films, hot-water systems, heating systems, cables, and wires. The presented work focused on a multi-stage study of the degraded PB-1 extrudates in two degradation modes: natural and artificial aging. The chemistry of the degradation and, subsequently, the degradation rate of the extrudates were studied. The acceleration time equivalent was used to determine the degradation rate between naturally and artificially aged extrudates. The effects of the degradation on the mechanical properties, namely tensile strength, tensile modulus, and elongation-at-break values were studied and compared to the development of the surface cracks.

## Experimental

### Materials and methods

Isotactic poly(1-butene) (PB-1) DP 0401 M was obtained from LyondellBasell (Louvain la Neuve, Belgium). According to information from the manufacturer, it was a semi-crystalline homopolymer with a balance between creep resistance and formation of cracks in an environment with increased temperature. The basic properties were a density of 0.915 $g.cm^{-3}$ (ISO 1183) and a melt flow index of 15 g/10 min (ISO 1133).

The material was extruded on a Brabender Plasti-Corder PL2000 single-screw extruder, and the process conditions were set as follows: screw compression ratio 1:4; screw speed 20 rpm; barrel temperatures of 135 °C, 140 °C, 145 °C, and

150 °C; extrusion slit die with profile 2×20 $mm^2$ with temperature 150 °C.

## Characterization

For tensile testing the dog-bone-shaped plates (ISO 527–3 type 5A) with a total length of 110 mm, weight of 3 g and the length of working distance 30 mm, width 6 mm and thickness 2 mm, naturally colored (no colorants were used) were cut from the extruded samples.

Artificial aging was performed in a SEPAP 12/24 MPC device (ATLAS company) equipped with four 400 W medium-pressure mercury arc lamps in borosilicate envelops that emit discrete radiation at 290, 313, 365, 405, 436, 547, and 579 nm, at a temperature of 60 °C, and at different irradiation time intervals (0, 10, 20, 40, and 60 h). A single sample, with a length of 50 mm and a weight of 1.5 g, along with six dog-bone-shaped samples for each specific exposure duration, were subjected to both artificial aging and natural weathering processes. One sample length of 50 mm, weight of 1.5 g, and six dog-bone-shaped samples for each individual exposition time were exhibited to artificial aging resp. natural weathering. Testing specimens were in the middle of the test chamber mounted on carousel.

The study of natural weathering was conducted in Nivnice, Czech Republic, which is situated at an altitude of 250 m with geographical coordinates 48°58′42″N latitude and 17°38′47″E longitude. During the period extending from July to September, specimens in a dog-bone shape were oriented toward the southern direction at an inclination of 45°. This setup facilitated the exposure of the samples to UV light exposure for a cumulative duration reaching up to 102 days. Meteorological data affecting the degradation process of naturally aged samples are given in Table 1.

A Nicolet 380 FTIR spectrometer, equipped with a SPECAC ATR Diamond-Germanium crystal, with a resolution of 4 $cm^{-1}$ and measuring 32 scans, was used for surface analysis of the degraded samples. Molecular degradation was characterized by the carbonyl index *CI* as follows:

$$CI = A_C/A_R,$$

where $A_C$ is the area of carbonyl absorption peaks (in the range of 1504–1816 $cm^{-1}$), and $A_R$ is the area of reference peaks unaffected by photo-oxidation and different degrees of crystallinity (in the range from 1400 to 1500 $cm^{-1}$) [17, 36].

The yellow index YI E313 was measured using an UltraScan Pro spectrophotometer from Hunterlab.

For wide-angle X-ray scattering in reflection mode, a Philips X'pert (PANalytical, Netherlands) was used with an interval of 2θ = 5–30°, a shift angle of 0.05°, and a duration 0.5 s. A monochromatic CuKα anode beam with a wavelength of $\lambda = 0.154$ nm and a Ni filter were used. The tetragonal phase of PB-1 (phase II) shows the following diffraction peaks at 11.9°, 16.9°, and 18.5° 2θ, corresponding to the (200), (220), and (213) planes, respectively. Hexagonal phase I is characterized by four distinct diffraction peaks of 10.0°, 17.5°, and 20.4° 2θ, originating from the (110), (300), (220 + 211) planes, respectively. It should be noted that due to the phase transition with increasing time, the intensity of the peaks typical of hexagonal phase I (i.e., (110) at 10.0° 2θ) increased, while the intensity of the peaks related to tetragonal phase II (i.e., (200) at 11.9° 2θ) decreased [37].

PEAKFIT v4 was used to evaluate crystallinity. From the point of view of phase transformation, it was more appropriate to observe the disappearance of the peak 2θ = 11.9° of phase II (reflection plane 200) rather than the increase of the peak in the region of 2θ = 10.0° of form I (reflection plane 110). A post-crystallization phenomenon occurred with the phase transformation, during which, part of the amorphous polymer crystallized into phase I [38–40]. The development of the peaks of the individual phases was observed (2θ angles 10.0° and 11.9°), and the ratio of the peak heights and the content of the given phase to the sum of both heights were subsequently calculated [41].

A Zwick 145,665 multi-purpose apparatus was used for the tensile test according to standard EN ISO 527–3. The specimens were stretched at room temperature until rupture at a test speed of 50 mm/min. For each measurement set, 5 specimens were used. The stress and strain values derived strength-at-break and elongation-at-break. In addition, the elastic modulus was evaluated using a Zwick external extensometer (gauge length of 20 mm) at a test speed of 1 mm/min (ISO).

**Table 1** Meteorological data affecting the naturally aged samples

| Month | Rain-fall (mm) | ∅T (°C) | Clearness day | Cloudiness day | Thunderstorm | Summer day | Tropic day |
|---|---|---|---|---|---|---|---|
| July | 104.7 | 19.7 | 10 | 14 | 8 | 12 | 10 |
| August | 95.3 | 18.9 | 14 | 1 | 12 | 18 | 7 |
| September | 62.3 | 13.7 | 9 | 9 | 1 | 9 | 3 |

∅T—average temperature (calculated by three temperatures at 7, 14, and 21 h; evening observation was calculated twice and divided by 4); clearness day—max 20% of the covered sky; cloudiness day—cloudy 80–100%; summer day—part of day > 25 °C; tropic day—part of day > 30 °C

The surface morphology of the degraded samples was examined using a scanning electron microscope (SEM) with an accelerating voltage of 10 kV (Phenom Pro desktop scanning electron microscope with the BSE detector, Phenom-World B.V., The Netherlands). No treatment of degraded samples has been applied.

## Results and discussion

### Changes in chemical composition

FTIR–ATR can identify the specific functional groups present in the degraded polymer, providing information about the degradation mechanism and the types of reactions. In this work, the carbonyl groups in the degraded polymer sample can indicate that the sample underwent oxidative degradation. The number of the presented carbonyl groups can be used to quantify the changes in the chemical structure of the polymer due to the degradation [17].

A comparison of the evolution of the carbonyl index and, thus, the chemical changes evoked by the degradation is shown in Fig. 1. In Fig. 1a, a, visual representation of the evolution of the carbonyl groups for natural weathering can be seen. In Fig. 1b, the evolution of the carbonyl groups for artificially aged samples is shown. Each curve represents a characteristic aging time 0, 24, 37, 58, 72, 88, and 102 days of natural weathering and 0, 10, 20, 40, and 60 h of artificial aging. In the artificially aged and naturally weathered samples, a gradual increase in the characteristic peak can be observed in the absorption region of the carbonyl groups at 1700–1750 $cm^{-1}$. An increase can also be observed in the region at 1645 $cm^{-1}$, which is attributed to vinyl groups. In the naturally weathered samples in the region of carbonyl groups, the most significant increase was observed after only 24 days of exposure. In all the naturally weathered samples, the significant formation of carboxylic acids was observed (1712 $cm^{-1}$).

A comparison of the properties of PB-1 in this work was based on the interpolation of the development of the carbonyl index values during artificial and natural weathering and the subsequent recalculation of the accelerated aging time according to the corresponding carbonyl index values to the equivalent time during natural weathering. This approach was based only on the development of the carbonyl index, which was primarily affected by photo-oxidation [10, 42]. Therefore, the contribution of the influence of humidity and temperature fluctuations was neglected, however, these fluctuations influenced the development of the material's mechanical properties. Figure 2 shows the evolution of the

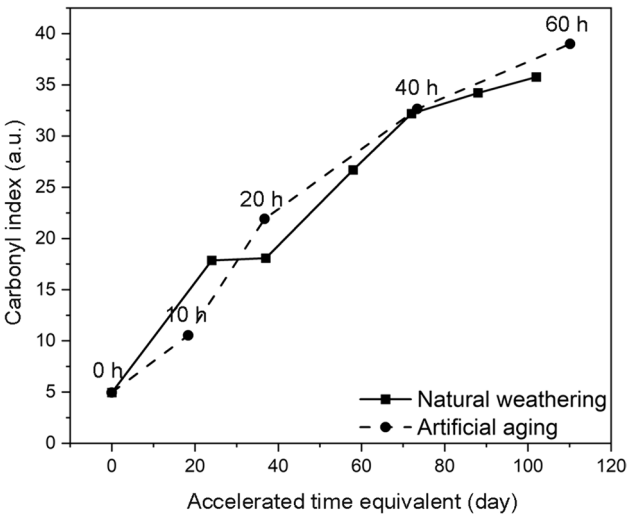


**Fig. 2** Comparison of the evolution of the carbonyl index of the artificially aged and naturally weathered PB-1 samples with the application of accelerated time equivalent

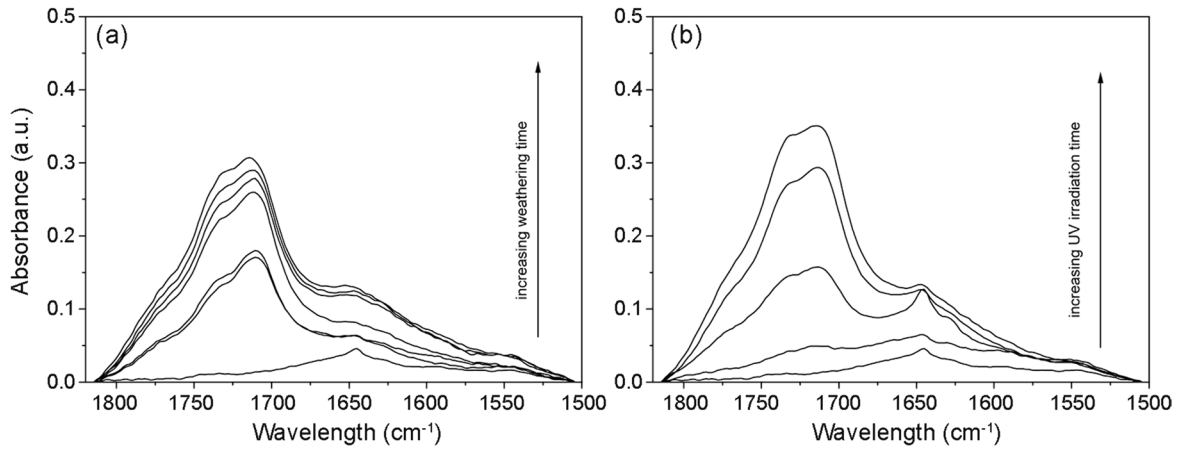


**Fig. 1** FTIR–ATR spectra of: **a** naturally weathered and **b** artificially aged PB-1 samples

carbonyl index as a function of the exposure time concerning the accelerated time equivalent.

The increase in carbonyl products was slower due to washing out of the sample surface due to weather conditions. On the other hand, in artificially irradiated samples, the content of chemical groups essentially increased throughout the exposure period, which may also lead to the erosion of the crystallites and possible breakdown of the material.

In Fig. 3, the development of yellow coloring during degradation can be observed. For both series, the trend was similar to the measured carbonyl index (Fig. 2). Based on this comparison, the yellow index (in the case of undyed polymers) indicated the degree of degradation [43]. The yellow index was higher in naturally weathered samples due to the presence of external influences not present during artificial aging, e.g., a higher amount of oxygen, rain, and changeable surrounding temperature, which resulted in different chemical degradation processes and formation of different chemical compounds; these conditions cannot be precisely defined due to the impossibility of deconvoluting the peaks in the range of carbonyls (Fig. 1).

## Changes in supermolecular structure

The development of crystallinity during the degradation of both sets is recorded in Fig. 4. It must be emphasized that both series of samples were prepared from the exact extrusion string. WAXS measurements were performed in reflection mode; although an increase in crystallinity in the sample's center might not be observable, higher crystallinity was expected in the surface layers, which was confirmed by the performed measurements. In both cases, the expected increase in crystallinity occurred due to the process

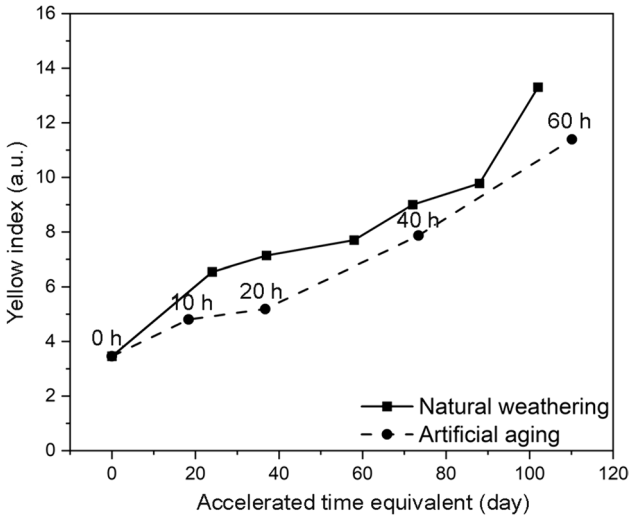


**Fig. 3** Yellow index of artificially aged and naturally weathered PB-1 samples with the application of accelerated time equivalent

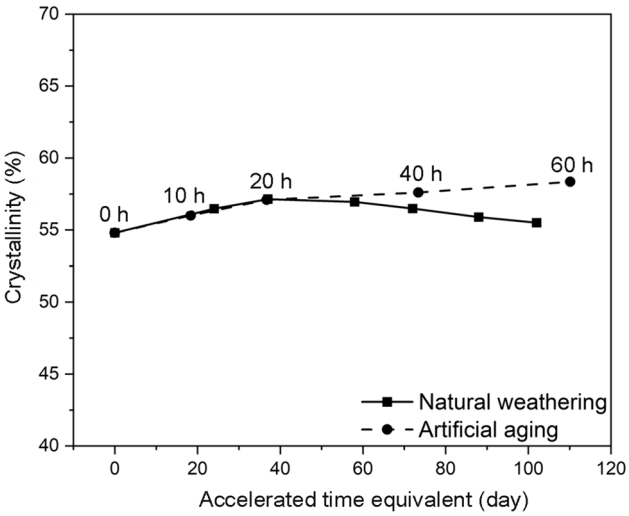


**Fig. 4** Development of crystallinity during the artificial aging and natural weathering of PB-1 samples with the application of accelerated time equivalent

of chemi-crystallization, as mentioned above. After 20 h of artificial aging (37 days of natural weathering), differences between the development of crystallinity were visible. When the samples were artificially aged, the crystallinity slightly raised. Increasing the time of natural weathering (more than 37 days) led to slight decrease in the crystallinity due to chain shortening.

Surface observation of the artificially aged samples is depicted in Fig. 5, from which it is evident that the visible surface cracks started to appear after 40 h of UV irradiation. The crack orientation was parallel to the extrusion direction. These parallel cracks were then perpendicularly connected, thus creating a cracked net after 60 h of irradiation; further UV irradiation led to wider cracks.

On the other hand, natural weathering led to a different crack initiation mechanism, leading to a higher quantity of more condensed initial cracks. The surface structure of the sample with most prolonged exposure to natural weathering (102 days) was consisted of high amounts of individual small cracks, which were only partially connected into wider and bigger cracks.

## Mechanical properties

Figures 6 – 8 show the evolution of the mechanical properties of the samples during aging. Compared to artificial aging, natural weathering led to different results in all three measured parameters (tensile modulus, tensile strength and elongation-at-break). In the case of the artificially aged samples, the tensile modulus gradually decreased from approximately 500 to 450 MPa, except for the initial 20 h of the measurement (Fig. 6). Conversely, in the case of the natural

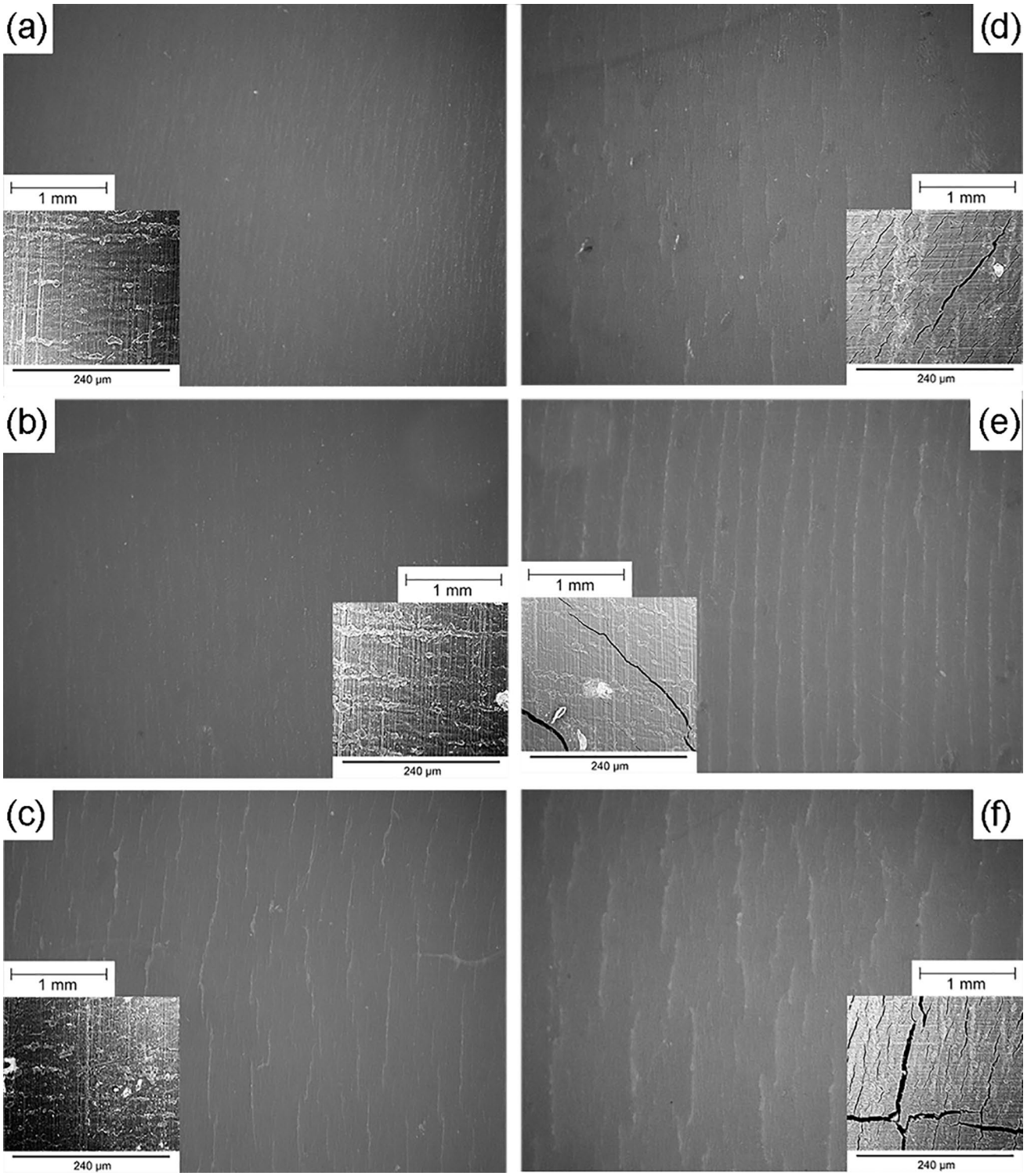


**Fig. 5** Stereomicroscopic and SEM micrographs of PB-1 samples subjected to a progressive degree of UV irradiation for: **a** 20, **b** 40, and **c** 60 h compared with those of naturally weathered samples for: **d** 37, **e** 72, and **f** 102 days related on the basis of the accelerated time equivalent

weathering, there was a slight increase in the modulus; the modulus values were partly corresponded to the samples artificially irradiated for 20 h. This phenomenon could be attributed to chemi-crystallization, where chain scission and rearrangement into crystalline domains occurred, explaining the slight increase in tensile modulus in the case

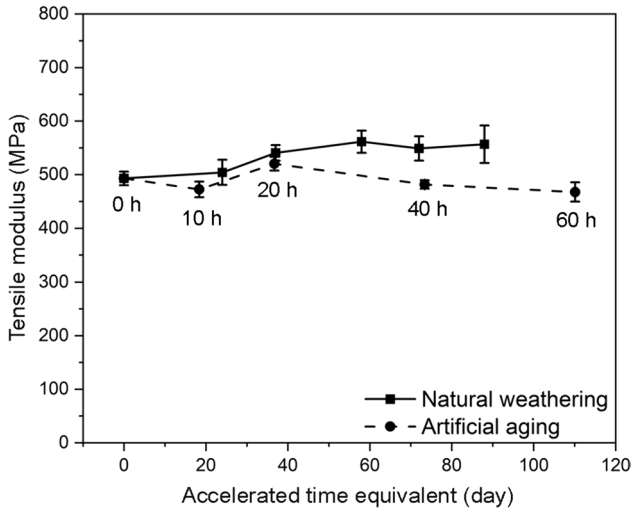


**Fig. 6** Development of the tensile modulus of the PB-1 samples during artificial aging and natural weathering with an accelerated time equivalent

of the accelerated UV aging. In natural weathering due to chemi-crystallization, the crystallinity increased in the first exposure phase (37 days). Then, it slowly decreased while remaining higher than it was at the beginning of exposure (Fig. 4).

Figure 7 shows the dependence of the tensile strength-at-break on the exposure time. As with the tensile modulus, there was again a slight increase in the tensile strength within the first 10 h of exposure for the artificially aged samples; again, this could be attributed to a slight increase in crystallinity. With an increasing exposure time, the decrease from 21 to 15 MPa occurred.

The first cracks were visible after 40 h of exposure, but at 20 h of exposure, the seeds of cracks must have been already formed in the samples (or shortened chains, caused a decrease in strength), while the subsequent aging caused a decrease in strength to 14.5 MPa. On the other hand, the tensile strength of the naturally aged samples slightly decreased after 24 days of exposure. However, after 37 days of exposure, the tensile strength drops to half of the original value; on this day, the cracks were not directly observable, but the chains of the sample were so shortened, that the tensile strength was dramatically reduced from 20 MPa to 10.5 MPa. In the following days, there was a slight decrease to approximate values of 8 to 9 MPa.

The development of elongation-at-break in the first 60 h of irradiation can be observed in Fig. 8. The radical downfall of elongation-at-break value was observed during the first 20 h of the UV irradiation, from 38% to merely 3% in the case of the naturally weathered sample and approximately 7% in the case of the artificially aged samples. Further irradiation has an almost negligible effect. Elongation hovered around 4% for naturally weathered samples and around 10% for artificially aged samples; it is necessary to consider that those values were shallow and could therefore be assumed as a minimum for irradiated samples. A faster decrease in elongation for naturally weathered samples could be resulted from temperature fluctuations and rain washing of the sample surface and, thus, accelerated the degradation process [21]. The fact that chemi-crystallization and chain shortening generally led to decreased ductility was consistent with findings in this work [44].

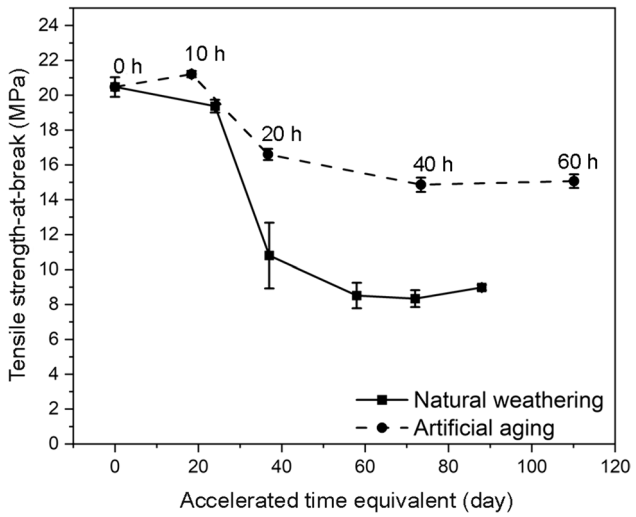


**Fig. 7** Development of tensile strength-at-break of PB-1 samples during artificial aging and natural weathering with an accelerated time equivalent

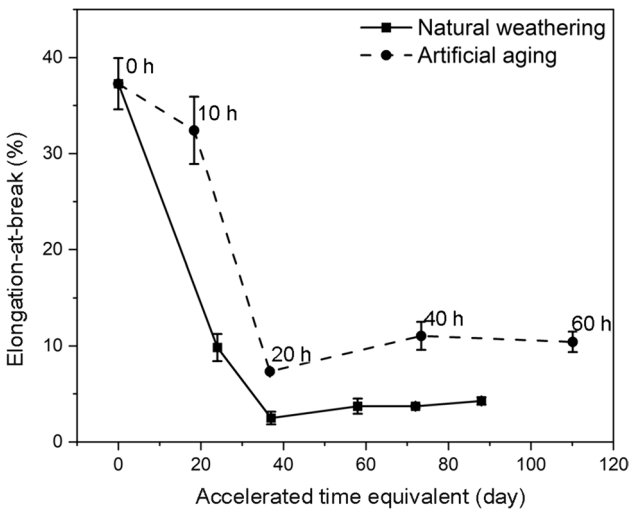


**Fig. 8** Development of elongation-at-break of PB-1 samples during artificial aging and natural weathering with an accelerated time equivalent

After comparing both aging methods, it was evident that individual aging conditions impacted the resulting properties of the degraded material. The most significant differences were on the surface of the examined samples, and those differences were projected into the mechanical properties in different ways. The naturally weathered samples were both more brittle than the artificially aged samples while having a higher tensile modulus [45]. Although there were almost no differences in the polymorphic structure of PB-1 and the total crystallinity was almost constant during the experiment, the surface changes induced by both degradation methods seemed to be the driving mechanism of the changes in the mechanical properties.

For the sake of the chemical product development during aging, the carbonyl index and yellow index provided an acceptable correlation and, thus, can be used to roughly estimate the material state of degradation in the initial period.

Comparison of the morphologies of the degraded surfaces via stereomicroscopy and SEM contributed to understanding the different trends in the mechanical behavior of the degraded samples. In natural weathering, the large number of minor cracks caused a significant decrease in strength and ductility. Concurrently, the lower energy of UV irradiation, cyclical day and night shifting, and rain/wind washing all contributed to the development of chemi-crystallization, thus maintaining the tensile modulus still relatively high. In contrast, the number of cracks created during artificial aging was lower; however, the cracks reached much larger dimensions, contributing to drop in the tensile modulus. The reasoning behind the lower number of initial cracks could be the surface that was oversaturated with chemical products of the degradation (aldehydes and ketones), which were not washed away, leading to the formation of a protective layer, and degradation was more pronounced in the deep and wide cracks [46].

## Conclusion

This work is the first to compare the degradation behavior of isotactic poly(1-butene) (PB-1) under artificial aging and natural weathering conditions, using accelerated time equivalent to correlate the final properties of the aged PB-1. It also investigated the effects of degradation on the mechanical properties, surface morphology, and crystalline structure of PB-1. The tailoring of the accelerated aging experiment led to slightly different mechanical behavior in the same material, mainly attributed to differences in crack development. During natural weathering, the chemi-crystallization phenomenon was observed, which led to an increase in the tensile modulus; on the other hand, during artificial aging, the material did not have enough time to supply different contaminants, and although its crystallinity slightly increased, the modulus decreased due to the size of the surface cracks. For both methods, the elongation-at-break and tensile strength values decreased, which was the expected outcome of any photo-oxidative process. Artificial aging predicted the behavior of naturally weathered material quite well and within an acceptable range of values. The only exception was the tensile strength-at-break value which was higher for the accelerated samples. However, the decrease was outside the acceptable range and general usability was still predicted correctly.

**Acknowledgements** This research was supported within the project IGA/FT/2023/008.

**Funding** Open access publishing supported by the National Technical Library in Prague. IGA/FT/2023/008, IGA/FT/2023/008, Sona Zenzingerová.

**Data availability** The datasets used and/or analyzed during the current study are available in digital form and can be accessed upon reasonable request. Please contact the corresponding author for data requests.

## Declarations

**Conflict of interest** The authors declare that they have no known competing financial interests or personal relationships that could have appeared to influence the work reported in this work.



## References

1. Harper CA (2006) Handbook of plastics technologies: the complete guide to properties and performance, 1st edn. McGraw-Hill, New York
2. Kaszonyiová M, Rybnikář F, Lapčík L, Vilčáková J (2021) The effect of long-term natural aging on the iPB-1 structure and the II – I phase transformation rate. Polym Degrad Stab 183:109437. https://doi.org/10.1016/j.polymdegradstab.2020.109437
3. Stolte I, Cavallo D, Alfonso GC, Portale G, Van Drongelen M, Androsch R (2014) Form I′ crystal formation in random butene-1/propylene copolymers as revealed by real-time X-ray scattering using synchrotron radiation and fast scanning chip calorimetry. Eur Polym J 60:22–32. https://doi.org/10.1016/j.eurpolymj.2014.08.011
4. Fu P, Li J, Jiang S (2020) Role of chain dynamics in crystal transition of isotactic polybutene-1. Polymer (Guildf) 210:123029. https://doi.org/10.1016/j.polymer.2020.123029

5. Cardew PT (2023) Ostwald Rule of Stages—Myth or Reality? Cryst Growth Des 23:3958–3969. https://doi.org/10.1021/acs.cgd.2c00141
6. Xin R, Zhang J, Sun X, Li H, Ren Z, Yan S (2018) Polymorphic behavior and phase transition of poly(1-butene) and its copolymers. Polymers (Basel) 10:556. https://doi.org/10.3390/polym10050556
7. Ailara DL (1975) Aging of polymers. Environ Health Perspect 11:29–33. https://doi.org/10.1289/ehp.751129
8. Koriem A, Ollick AM, Elhadary M (2021) The effect of artificial weathering and hardening on mechanical properties of HDPE with and without UV stabilizers. Alex Eng J 60:4167–4175. https://doi.org/10.1016/J.AEJ.2021.03.024
9. Fairbrother A, Hsueh H-C, Kim JH, Jacobs D, Perry L, Goodwin D, White C, Watson S, Sung L-P (2019) Temperature and light intensity effects on photodegradation of high-density polyethylene. Polym Degrad Stab 165:153–160. https://doi.org/10.1016/j.polymdegradstab.2019.05.002
10. Grause G, Chien M-F, Inoue C (2020) Changes during the weathering of polyolefins. Polym Degrad Stab 181:109364. https://doi.org/10.1016/j.polymdegradstab.2020.109364
11. Craig IH, White JR, Shyichuk A, v., Syrotynska I, (2005) Photo-induced scission and crosslinking in LDPE, LLDPE, and HDPE. Polym Eng Sci 45:579–587. https://doi.org/10.1002/pen.20313
12. Babaghayou MI, Mourad AHI, Lorenzo V, de la Orden MU, Martínez Urreaga J, Chabira SF, Sebaa M (2016) Photodegradation characterization and heterogeneity evaluation of the exposed and unexposed faces of stabilized and unstabilized LDPE films. Mater Des 111:279–290. https://doi.org/10.1016/j.matdes.2016.08.065
13. Makki M, Ayoub G, Pannier C, Dargazany R, Kadri R, Abdelaziz MN, Nouri H (2023) Micromechanical modeling of the visco-hyperelastic–viscoplastic behavior and fracture of aged semicrystalline polymers. Int J Non Linear Mech 155:104456. https://doi.org/10.1016/j.ijnonlinmec.2023.104456
14. Rodriguez AK, Mansoor B, Ayoub G, Colin X, Benzerga AA (2020) Effect of UV-aging on the mechanical and fracture behavior of low density polyethylene. Polym Degrad Stab 180:109185. https://doi.org/10.1016/j.polymdegradstab.2020.109185
15. Batista NL, Rezende MC, Botelho EC (2018) Effect of crystallinity on CF/PPS performance under weather exposure: moisture, salt fog and UV radiation. Polym Degrad Stab 153:255–261. https://doi.org/10.1016/j.polymdegradstab.2018.03.008
16. Gallo R, Severini F (2013) Course of the changes in thick and thin isotactic polypropylene samples subjected to natural aging. Polym Degrad Stab 98:1144–1149. https://doi.org/10.1016/j.polymdegradstab.2013.03.017
17. Obadal M, Čermák R, Raab M, Verney V, Commereuc S, Fraïsse F (2006) Study on photodegradation of injection-moulded β-polypropylenes. Polym Degrad Stab 91:459–463. https://doi.org/10.1016/j.polymdegradstab.2005.01.046
18. Wu H, Zhao Y, Dong X, Su L, Wang K, Wang D (2021) Probing into the microstructural evolution of isotactic polypropylene during photo-oxidation degradation. Polym Degrad Stab 183:109434. https://doi.org/10.1016/j.polymdegradstab.2020.109434
19. Tian R, Li K, Lin Y, Lu C, Duan X (2023) Characterization Techniques of Polymer Aging: From Beginning to End. Chem Rev 123:3007–3088. https://doi.org/10.1021/acs.chemrev.2c00750
20. Shirazi RN, Aldabbagh F, Ronan W, Erxleben A, Rochev Y, McHugh P (2016) Effects of material thickness and processing method on poly(lactic-co-glycolic acid) degradation and mechanical performance. J Mater Sci Mater Med 27:154. https://doi.org/10.1007/s10856-016-5760-z
21. Wypych G (2018) Handbook of material weathering, 6th edn. ChemTec Publishing, Toronto, Canada
22. Ye L, Liu M, Huang Y, Zhang Z, Yang J (2015) Effects of molecular weight on thermal degradation of poly(α-methyl styrene) in nitrogen. J Macromol Sci Part B 54:1479–1494. https://doi.org/10.1080/00222348.2015.1094645
23. Madras G, Chung GY, Smith JM, McCoy BJ (1997) Molecular weight effect on the dynamics of polystyrene degradation. Ind Eng Chem Res 36:2019–2024. https://doi.org/10.1021/ie9607513
24. Jerdy AC, Pham T, González-Borja MÁ, Atallah P, Soules D, Abbott R, Lobban L, Crossley S (2023) Impact of the presence of common polymer additives in thermal and catalytic polyethylene decomposition. Appl Catal B 325:122348. https://doi.org/10.1016/j.apcatb.2022.122348
25. Burelo M, Gaytán I, Loza-Tavera H, Cruz-Morales JA, Zárate-Saldaña D, Cruz-Gómez MJ, Gutiérrez S (2022) Synthesis, characterization and biodegradation studies of polyurethanes: Effect of unsaturation on biodegradability. Chemosphere 307:136136. https://doi.org/10.1016/j.chemosphere.2022.136136
26. Ho K-LG, Pometto AL, Hinz PN (1999) Effects of temperature and relative humidity on polylactic acid plastic degradation. J Environ Polym Degrad 7:83–92. https://doi.org/10.1023/A:1021808317416
27. Massey S, Adnot A, Rjeb A, Roy D (2007) Action of water in the degradation of low-density polyethylene studied by X-ray photoelectron spectroscopy. Express Polym Lett 1:506–511. https://doi.org/10.3144/expresspolymlett.2007.72
28. Samarth NB, Mahanwar PA (2021) Degradation of polymer & elastomer exposed to chlorinated water—a review. Open J Org Polym Mater 11:1–50. https://doi.org/10.4236/ojopm.2021.111001
29. Loh XJ (2013) The effect of pH on the hydrolytic degradation of poly(ε-caprolactone)-block-poly(ethylene glycol) copolymers. J Appl Polym Sci. https://doi.org/10.1002/app.37712
30. Qian S, Igarashi T, Nitta K-H (2011) Thermal degradation behavior of polypropylene in the melt state: molecular weight distribution changes and chain scission mechanism. Polym Bull 67:1661–1670. https://doi.org/10.1007/s00289-011-0560-6
31. Gijsman P, Fiorio R (2023) Long term thermo-oxidative degradation and stabilization of polypropylene (PP) and the implications for its recyclability. Polym Degrad Stab 208:110260. https://doi.org/10.1016/J.polymdegradstab.2023.110260
32. Gogotov IN, Barazov SKh (2014) The effect of ultraviolet light and temperature on the degradation of composite polypropylene. Int Polym Sci Technol 41:55–58. https://doi.org/10.1177/0307174X1404100313
33. Gijsman P, Meijers G, Vitarelli G (1999) Comparison of the UV-degradation chemistry of polypropylene, polyethylene, polyamide 6 and polybutylene terephthalate. Polym Degrad Stab 65:433–441. https://doi.org/10.1016/S0141-3910(99)00033-6
34. Gorelik BA, Kolganova IV, Matisová-Rychlá L, Listvojb GI, Drabkina AM, Golnik AG (1993) Effect of oxygen on the degradation of polypropylene initiated by ionizing irradiation. Polym Degrad Stab 42:263–266. https://doi.org/10.1016/0141-3910(93)90222-5
35. Elmanovich IV, Stakhanov AI, Zefirov VV, Pavlov AA, Lokshin BV, Gallyamov MO (2020) Thermal oxidation of polypropylene catalyzed by manganese oxide aerogel in oxygen-enriched supercritical carbon dioxide. J Supercrit Fluids 158:104744. https://doi.org/10.1016/j.supflu.2019.104744
36. Wu H, Zhao Y, Su L, Wang K, Dong X, Wang D (2021) Markedly improved photo-oxidation stability of α form isotactic polypropylene with nodular morphology. Polym Degrad Stab 189:109595. https://doi.org/10.1016/j.polymdegradstab.2021.109595
37. Xin R, Li Y, Shen H, Hu J, Wang S, Zhang H, Yan S (2022) The II to I phase transition of isotactic poly(1-butene) single crystals at an early stage. Macromolecules 55:8203–8209. https://doi.org/10.1021/acs.macromol.2c00836

38. Lauritzen JI, Hoffman JD (1973) Extension of theory of growth of chain-folded polymer crystals to large undercoolings. J Appl Phys 44:4340–4352. https://doi.org/10.1063/1.1661962
39. Looijmans S, Menyhard A, Peters GWM, Alfonso GC, Cavallo D (2017) Anomalous temperature dependence of isotactic polypropylene α-on-β cross-nucleation kinetics. Cryst Growth Des 17:4936–4943. https://doi.org/10.1021/acs.cgd.7b00872
40. Caelers HJM, Govaert LE, Peters GWM (2016) The prediction of mechanical performance of isotactic polypropylene on the basis of processing conditions. Polymer (Guildf) 83:116–128. https://doi.org/10.1016/j.polymer.2015.12.001
41. Kaszonyiová M, Rybnikář F (2019) The effect of some physical factors on the II → I Phase transition of isotactic polybutene-1. J Macromol Sci B 58:689–721. https://doi.org/10.1080/00222348.2019.1642549
42. Celina MC, Linde E, Martinez E (2021) Carbonyl identification and quantification uncertainties for oxidative polymer degradation. Polym Degrad Stab 188:109550. https://doi.org/10.1016/j.polymdegradstab.2021.109550
43. Mayer-Trzaskowska P, Robakowska M, Gierz Ł, Pach J, Mazur E (2024) Observation of the effect of aging on the structural changes of polyurethane/polyurea coatings. Polymers (Basel) 16:23. https://doi.org/10.3390/polym16010023
44. Majewski K, Mantell SC, Bhattacharya M (2020) Relationship between morphological changes and mechanical properties in HDPE films exposed to a chlorinated environment. Polym Degrad Stab 171:109027. https://doi.org/10.1016/j.polymdegradstab.2019.109027
45. Yamasaki RS (1984) Characterization of wet and dry periods of plastic surfaces during outdoor exposure. Durab Build Mater 2:155–169
46. Schoolenberg GE, Meijer HDF (1991) Ultra-violet degradation of polypropylene: 2. Residual strength and failure mode in relation to the degraded surface layer. Polymer (Guildf) 32:438–444. https://doi.org/10.1016/0032-3861(91)90447-Q